



# Application potential of grapefruit peel as dye sorbent: Kinetics, equilibrium and mechanism of crystal violet adsorption

Asma Saeed<sup>a,\*</sup>, Mehwish Sharif<sup>b</sup>, Muhammad Iqbal<sup>a</sup>

<sup>a</sup> Environmental Biotechnology Group, Biotechnology and Food Research Centre, PCSIR Laboratories Complex, Ferozpur Road, Lahore 54600, Pakistan

<sup>b</sup> School of Biological Sciences, University of the Punjab, Lahore 54590, Pakistan

## ARTICLE INFO

### Article history:

Received 16 November 2009

Received in revised form 20 February 2010

Accepted 10 March 2010

Available online 16 March 2010

### Keywords:

Dye sorption

Grape fruit peel

Crystal violet

Fixed-bed column

## ABSTRACT

This study reports the sorption of crystal violet (CV) dye by grapefruit peel (GFP), which has application potential in the remediation of dye-contaminated wastewaters using a solid waste generated by the citrus fruit juice industry. Batch adsorption of CV was conducted to evaluate the effect of initial pH, contact time, temperature, initial dye concentration, GFP adsorbent dose, and removal of the adsorbate CV dye from aqueous solution to understand the mechanism of sorption involved. Sorption equilibrium reached rapidly with 96% CV removal in 60 min. Fit of the sorption experimental data was tested on the pseudo-first and pseudo-second-order kinetics mathematical equations, which was noted to follow the pseudo-second-order kinetics better, with coefficient of correlation  $\geq 0.992$ . The equilibrium process was well described by the Langmuir isotherm model, with maximum sorption capacity of  $254.16 \text{ mg g}^{-1}$ . The GFP was regenerated using 1 M NaOH, with up to 98.25% recovery of CV and could be reused as a dye sorbent in repeated cycles. GFP was also shown to be highly effective in removing CV from aqueous solution in continuous-flow fixed-bed column reactors. The study shows that GFP has the potential of application as an efficient sorbent for the removal of CV from aqueous solutions.

© 2010 Elsevier B.V. All rights reserved.

## 1. Introduction

The global problem of clean water shortage has been exacerbated by its pollution caused through discharge of untreated industrial effluents. The problem is further aggravated in developing countries owing to uncontrolled population growth, and the use of outdated practices and technologies that consume large volumes of water in agricultural and industrial operations [1]. Several industrial processes utilize toxic chemicals for the manufacture of finished products, the unused parts of which escape into the environment as industrial waste-wash [2]. Environmental scientists worldwide are thus faced with the daunting task of developing cost-effective and efficient technologies for their treatment for miscellaneous human activities [3]. Discharge of industrial effluents containing hazardous contaminants, such as phenolics, toxic metals and dyes, even at low concentrations, are a cause of negative impact on the environment [4,5]. Out of the various pollutants, dyes rank among the most notorious organic contaminants that are discharged into the environment during textile, leather, paints, paper and dye manufacturing [5,6]. These are synthetic, water soluble and dispersible organic compounds, which may adversely

affect aquatic flora and fauna by reducing light penetration through water surface and their toxic effects, thus causing severe damage to aquatic biota [7]. Dyes are extremely stable due to their complex aromatic molecular structure, and are thus difficult to biodegrade [8,9]. From the aspect of environmental safety, the removal of synthetic dyes from the industrial waste-wash is of serious concern, since some dyes and their degradation products are toxic and carcinogenic [4,10]. Various conventional technologies, such as chemical oxidation and reduction, physical precipitation and flocculation, photolysis, adsorption, electrochemical treatment, reverse osmosis, bioaccumulation, and/or biodegradation, have been investigated for their removal from wastewaters [11,12]. Most of these methods, nevertheless, pose techno-economical limitations for field-scale applications [13].

Crystal violet dye, a member of the triphenylmethane group, is extensively used in animal and veterinary medicine as a biological stain, for identifying the bloody fingerprints being a protein dye, and in various commercial textile operations [14]. It is carcinogenic and has been classified as a recalcitrant molecule since it is poorly metabolized by microbes, is non-biodegradable, and can persist in a variety of environments [11]. Its removal from wastewaters before their discharge is, therefore, essential for environmental safety. Adsorption has been reported to be efficient and economical for the treatment of wastewaters containing dyes, pigments and other colourants [13]. Granular activated carbon has been used successfully, but is cost-prohibitive [15]. This has led to search for

\* Corresponding author. Tel.: +92 42 99230688; fax: +92 42 99230705.  
E-mail address: [asmadr@wol.net.pk](mailto:asmadr@wol.net.pk) (A. Saeed).

cheaper adsorbent substitutes derived from agricultural and wood wastes [4]. As a result, activated carbon made from male flowers of coconut [14], rice husk [16] and flame tree (*Delonix regia*) pods [4], and acid-treated neem (*Azadirachta indica*) sawdust [5] and almond skin [9], have been studied for the sorption of crystal violet. These adsorbents either involve cost-input pretreatments or are not abundantly available as wastes. The present report attempts to eliminate such preparatory steps and limitations of availability by using raw grapefruit peel, a waste generated in abundance during industrial processing of the fruit.

Grapefruit is cultivated in all tropical and subtropical regions of the world, with approximately 4 million metric tons annual production [17]. Thus, a lot of grapefruit peel (GFP) is available throughout the world. GFP contains several water soluble and insoluble monomers and polymers [18,19]. The water soluble fraction contains glucose, fructose, sucrose and some xylose, while pectin, cellulose, hemicellulose and lignin constitute between 50% and 70% of the insoluble fraction. These polymers are rich in carboxyl and hydroxyl functional groups, which may bind cationic dye molecules in aqueous solution [20]. The present work was undertaken to evaluate the application potential of the pectin- and cellulose-rich GFP as an inexpensive and environment-friendly adsorbent for treating wastewaters containing the cationic crystal violet (CV) dye. The study is further unique as there is no existing report for the removal of any dye by GFP. Parameters investigated for sorption of the dye included the effect of temperature, pH, biomass dose, and dye concentration. FTIR analysis was done to identify the functional groups present in the grapefruit peel, and dye desorption was done to determine reuseability of the sorbent peel for a number of repeated applications. An attempt has been made to interpret the data, based on ion exchange mechanism, and for finding a fit on various kinetics and isotherms equations.

## 2. Material and methods

### 2.1. Sorbent material

Grapefruit peel was collected from the local fresh fruit juice vending outlets. The GFP was sorted by removing leaves, twigs and other debris immediately after collection. After thorough washing with tapwater, GFP was washed with double distilled water, oven dried at  $70 \pm 2^\circ\text{C}$ , ground, and sieved. Powdered GFP of particle size 0.85–1.0 mm was used for the sorption studies.

### 2.2. Crystal violet stock solution

Crystal violet, a basic dye, C.I. 42555,  $\lambda_{\text{max}} = 586 \text{ nm}$ , molecular formula  $\text{C}_{25}\text{H}_{30}\text{N}_3\text{Cl}$ , also known as hexamethyl pararosaniline chloride, was purchased from Fluka, Darmstadt, Germany and its chemical structure is shown in Fig. 1. Stock solution of  $1000 \text{ mg L}^{-1}$  crystal violet was prepared by dissolving  $1.0 \text{ g L}^{-1}$  of the dye in

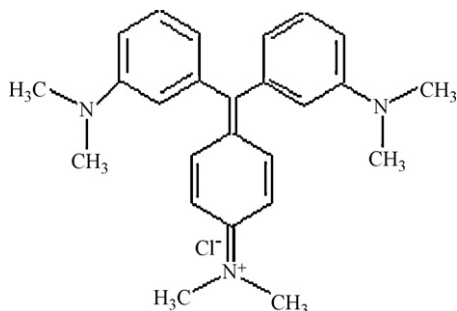


Fig. 1. Chemical structure of crystal violet.

ultrapure deionized water ( $18 \text{ M}\Omega \text{ cm}$ ). The dye solution pH was adjusted using 0.1 N HCl or 0.1 N NaOH. Fresh dilutions of the desired dye concentrations were made at the start of each experiment.

### 2.3. Sorption procedure for equilibrium and kinetics studies

The maximum sorption capacity was determined by contacting 100 mL crystal violet solution of known concentrations ( $5\text{--}600 \text{ mg L}^{-1}$ , pH 6.0) in 250-mL Erlenmeyer flasks. The flasks, tightly stoppered, were shaken on orbital shaker at 100 rpm at ambient temperature ( $30 \pm 2^\circ\text{C}$ ) for 60 min to ensure establishment of equilibrium. The GFP was separated by centrifugation at 5000 rpm for 5 min. Residual concentration of crystal violet was determined spectrophotometrically (Shimadzu spectrophotometer UV-Vis 1700, Japan) at 585 nm. Dilutions were made when absorbance exceeded 1.5. The effect of initial pH was determined by varying dye solution pH in the range 2–10. Biomass concentration was optimized by varying GFP dose ( $0.1\text{--}3.0 \text{ g L}^{-1}$ ). Dye-free solution (double distilled water) was used as control. The effect of temperature on sorption was determined at 20, 30 and  $45^\circ\text{C}$ . The amount of crystal violet sorbed onto GFP,  $q_e$  ( $\text{mg g}^{-1}$ ), was calculated using the equation:

$$q_e = \frac{(C_i - C_e)V}{W} \quad (1)$$

where  $q_e$  is the crystal violet uptake ( $\text{mg dye g}^{-1}$  sorbent);  $C_i$  and  $C_e$  are, respectively, the initial and equilibrium liquid-phase concentrations of crystal violet ( $\text{mg L}^{-1}$ );  $V$  the volume of crystal violet solution (L); and  $W$  the weight of GFP (g).

For determining the optimum contact time for sorption equilibrium and kinetics of sorption, the sorbate–sorbent were contacted for various time intervals (10–240 min). The residual dye concentration was determined and the amount of crystal violet sorbed, at time  $t$  was calculated using the equation:

$$q_t = \frac{(C_i - C_e)V}{W} \quad (2)$$

where  $q_t$  is the crystal violet uptake at time  $t$  ( $\text{mg dye g}^{-1}$  sorbent).

### 2.4. Desorption and reuse of regenerated sorbents

The CV-loaded biomass of GFP, which was initially exposed to  $100 \text{ mg L}^{-1}$  of CV at pH 6.0 and  $30^\circ\text{C}$ , was contacted with 50 mL of 1 M NaOH as the dye-desorbing agent for 60 min on a rotary shaker at 100 rpm. The GFP biomass was removed by centrifugation and the quantity of crystal violet dye recovered was determined. After desorption, the GFP was washed several times with double distilled water and the regenerated GFP was reused for the next adsorption cycle following the same procedure as employed in the adsorption equilibrium experiments.

### 2.5. FTIR analysis

FTIR spectrophotometer (ThermoNicolet IR-100 spectrometer, ThermoNicolet Corporation, Madison, USA) was used to identify the chemical functional groups present on the native GFP. IR absorbance data were obtained for wavenumbers in the range of  $400\text{--}4000 \text{ cm}^{-1}$  and analyzed using Encompass<sup>®</sup> software provided by the FTIR spectrophotometer manufacturer. For obtaining FTIR spectra, ball-milled GFP biomass was mixed with KBr (ratio 1:100), compacted into a tablet form using a bench press, and the material was run for obtaining FTIR spectra.

## 2.6. Column studies

A glass column, 1.7 cm in diameter  $\times$  25 cm in height, was packed with  $14 \pm 0.56$  GFP having 20 cm bed-height. CV solution of known concentration ( $50 \text{ mg L}^{-1}$  or  $100 \text{ mg L}^{-1}$ , pH 6.0) was then pumped upwards through the column at a flow rate of  $2.5 \text{ mL min}^{-1}$ . Samples were collected at regular intervals from the effluent to measure residual CV concentrations. As the bed was saturated, the CV loading was terminated. The total amount of CV uptake by the GFP-packed column was calculated according to the mass balance of dye expressed as:

$$q = \frac{V(C_i - C_{eq})}{M} \quad (3)$$

where  $V$  is the volume of dye solution (L) passed through the column;  $C_i$  the concentration of dye in the inlet solution;  $C_{eq}$  the dye concentration of solution at outlet of the column; and  $M$  the amount of GFP (g) packed in column.

## 2.7. Reproducibility and data analysis

Unless indicated otherwise, the data reported are the mean values of three separate experiments. The amount of dye adsorbed per unit biomass ( $\text{mg dye g}^{-1}$  GFP) was determined as shown in Eq. (1). Langmuir and Freundlich models [21,22] were used for the evaluation of sorption data. Langmuir isotherm assumes monolayer adsorption, which is presented by the equation:

$$q_{eq} = \frac{q_{max} b C_{eq}}{(1 + b C_{eq})} \quad (4)$$

where  $q_{eq}$  and  $q_{max}$  are the equilibrium and maximum dye uptake capacities ( $\text{mg g}^{-1}$  sorbent), respectively;  $C_{eq}$  the equilibrium dye concentration ( $\text{mg L}^{-1}$ ); and  $b$  the Langmuir equilibrium constant ( $\text{L mg}^{-1}$ ).

Freundlich model is presented as:

$$q_{eq} = K_F C_{eq}^{1/n} \quad (5)$$

where  $K_F$  and  $n$  are the Freundlich constants characteristic of the system.

In order to examine the controlling mechanism of the sorption process, such as mass transfer and chemical reaction, the pseudo-first-order, the pseudo-second-order, and intraparticle diffusion models were used to test the fit of experimental data of dye sorption by GFP on the kinetics equations proposed by various authors. The pseudo-first-order rate equation of Lagergren [23] is presented as:

$$\ln(q_{eq} - q_t) = \ln q_{eq} - k_{1ad} t \quad (6)$$

where  $k_{1ad}$  ( $\text{min}^{-1}$ ) is the pseudo-first-order reaction rate constant.

The pseudo-first-order considers the rate of occupation of sorption sites to be proportional to the number of unoccupied sites. A straight line of  $\ln(q_{eq} - q_t)$  versus  $t$  indicates the application of pseudo-first-order kinetics model. In a true pseudo-first-order process,  $\ln q_{eq}$  should be equal to the intercept of a plot of  $\ln(q_{eq} - q_t)$  against  $t$ . The pseudo-second-order equation [24], another equation used for kinetics analysis, which is based on the sorption equilibrium capacity, may be expressed in the following form:

$$\frac{t}{q_t} = \frac{1}{k_{2ad} q_{eq}^2} + \frac{1}{q_{eq}} t \quad (7)$$

where  $k_{2ad}$  is the pseudo-second-order rate equilibrium constant ( $\text{g mg}^{-1} \text{ min}^{-1}$ ).

A plot of  $t/q_t$  against  $t$  should give a linear relationship for the applicability of the pseudo-second-order kinetics model.

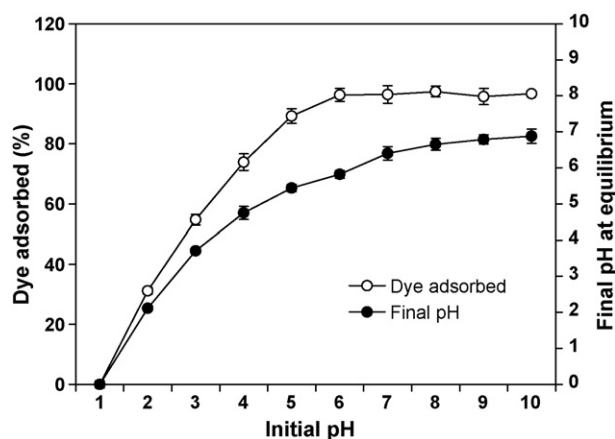


Fig. 2. Effect of initial pH on the sorption of crystal violet by grapefruit peel waste.

## 3. Results and discussion

### 3.1. Effect of pH on dye sorption

The pH of an aqueous solution is an important factor in dye adsorption, as it affects the surface charge of the sorbent material and the degree of ionization of the dye molecule [4]. pH has been related with changes in the structural stability and colour intensity of the dye molecule [6]. The removal of CV by GFP over a range of 2–10 was noted to increase with the increase in pH of the dye solution, appreciably up to pH 6.0 (Fig. 2). A further increase in dye sorption between pH 6.0 and 10 was insignificant. Since the optimum pH for dye biosorption by GFP was found to be 6.0, this pH was used for further studies. As the pH increases, the charge density of the dye solution decreases, so that electrostatic repulsion between the positively charged dye molecule and the surface of the adsorbent is lowered [6], which results in an increase in the sorption of the dye. The minimum removal of CV was thus found at pH 2, which is probably due to the  $\text{H}^+$  ions competing favourably with the cationic groups of the dye molecule for sorption sites on GFP biomass [6]. Similar observations have been reported by other authors [4,6]. The insignificant higher removal of the dye, observed at pH between 6 and 10, was noted to be accompanied by a drop in the original pH of the dye solution at sorption equilibrium. This indicates a cationic exchange process between the dye molecule and the GFP biomass with the release of protons ( $\text{H}^+$ ), as suggested in an earlier study [25].

### 3.2. Effect of contact time

The rate of sorption of CV by GFP was determined by contacting  $25 \text{ mg L}^{-1}$  of the CV solution (pH 6.0) with  $1.0 \text{ g L}^{-1}$  GFP for different intervals of time. The equilibrium was reached within 60 min of the sorbate–sorbent contact (Fig. 3). The uptake of CV, as a function of time, was noted to occur in two phases. The first phase involved a rapid uptake of dye during the first 20 min of the sorbate–sorbent contact, which was followed by a slow phase of dye removal spread over a significantly longer period of time (>60 min) until the equilibrium was reached. The two-stage sorption, the first rapid and quantitatively predominant and the second slower and quantitatively insignificant, has been extensively reported in literature [26]. The rapid stage, furthermore, may last for several minutes to a few hours, while the slow one continues for several hours to a day [27]. The rapid phase is probably due to the abundant availability of active sites on the sorbent, whereas with the gradual occupancy of these sites the sorption process becomes less efficient during the slower phase [28].

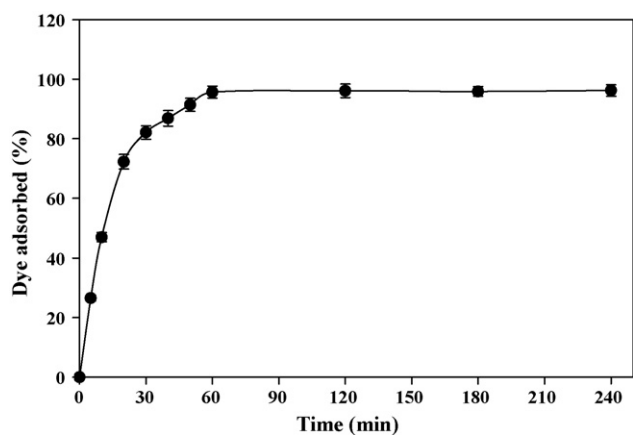


Fig. 3. Biosorption of crystal violet by grapefruit waste as a function of time.

### 3.3. Effect of temperature on dye adsorption

Effect of temperature on the adsorption of CV by GFP at equilibrium was investigated at three different temperatures, viz., 20 °C, 30 °C and 45 °C at the initial CV concentration of 25 and 100 mg L<sup>-1</sup>, pH 6.0 and the adsorbent dose of 1.0 g L<sup>-1</sup> (Fig. 4). The adsorption of CV was noted to enhance with the increase in temperature indicating that higher temperature favoured the removal of dye by sorption onto GFP. The observation is in agreement with the earlier report on the adsorption of CV by activated carbon from rice husk [16]. The enhanced adsorption at higher temperatures was suggested to be due to increase in the availability of active surface sites, increased porosity, and in the total pore volume of the adsorbent. These authors further suggested that the enhancement in adsorption may also be a result of an increase in the mobility of the dye molecule with an increase in their kinetic energy, enhanced rate of intraparticulate diffusion of the sorbate dye, and due to decrease in thickness of the boundary layer surrounding the sorbate dye at higher temperature so that the mass transfer resistance of the sorbate in the boundary layer decreases. The observations on the adsorption of CV on GFP in the present study further suggest that it was an endothermic process and may involve not only physical but also chemical sorption, as suggested in an earlier study on the adsorption of CV by activated carbon derived from male flowers of coconut tree [14].

### 3.4. Effect of the solid sorbent to the liquid sorbate ratio on CV adsorption

One of the parameters that strongly affect sorption capacity is the quantity of the contacting sorbent in the liquid phase [26].

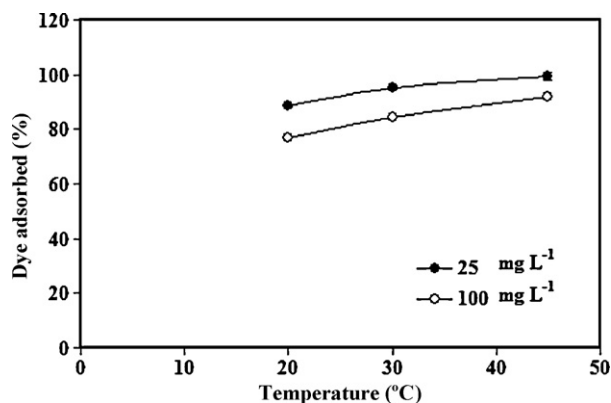


Fig. 4. Effect of temperature on the equilibrium sorption capacity of grapefruit peel.

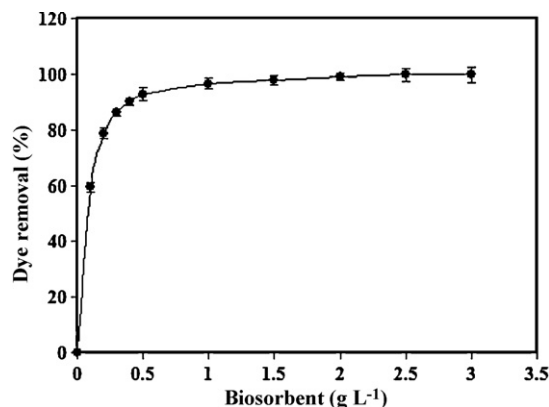


Fig. 5. Effect of grapefruit peel waste dosage on the sorption of crystal violet.

The influence of the solid sorbent to the liquid sorbate ratio on the sorption capacity of GFP was investigated at the constant initial concentration of CV 25 mg L<sup>-1</sup> (liquid phase), whereas the GFP mass (solid phase) was varied between 0.1 g L<sup>-1</sup> and 3.0 g L<sup>-1</sup>. The results obtained during the study show that increase in the solid phase mass from 0.1 g L<sup>-1</sup> to 1.0 g L<sup>-1</sup> resulted in a rapid increase in the uptake of CV (Fig. 5). Further increase in the solid phase mass from 1.0 g L<sup>-1</sup> to 3.0 g L<sup>-1</sup>, however, did not result in any appreciable increase in the sorption capacity of GFP. Therefore, the solid phase mass of 1.0 g L<sup>-1</sup> was selected for further studies. It may be concluded from these observations that at lower GFP dosage of <1.0 g L<sup>-1</sup>, the dye molecules were competing for sorption at limiting sorption sites. Therefore, as the quantity of GFP was increased from 0.1 g L<sup>-1</sup> to 1.0 g L<sup>-1</sup>, the availability of sorption sites eased resulting in greater percentage removal of the dye. The insignificant increase in the uptake of dye at the GFP dosage higher than 1.0 g L<sup>-1</sup> may be attributed to the presence of excess/surplus dye-binding sites on GFP than the available dye molecules present in the solution at the fixed concentration of 25 mg L<sup>-1</sup>. These observations are in agreement with those reported previously by other researchers for the sorption of dyes by different biological materials [7,13].

### 3.5. Effect of initial dye concentration on CV sorption

Dye adsorption capacity of GFP, as a function of initial concentration of dye within the aqueous solution is shown in Fig. 6. The initial concentration of dye was changed in the range of 10–600 mg L<sup>-1</sup>. The amount of dye adsorbed per unit mass of the adsorbent increased with increase in the initial concentration of CV. In order to reach the plateau values, which represent saturation

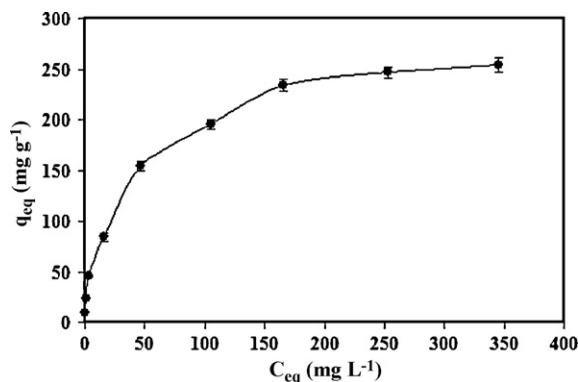


Fig. 6. Effect of initial dye concentration on crystal violet biosorption by grapefruit peel waste.



of the active sites on the sorbent, that is, the maximum adsorption capacity of the adsorbent, the initial concentration of CV was increased up to 600 mg L<sup>-1</sup>. As may be noted from Fig. 6, the maximum amount of dye adsorbed on GFP was 254 mg g<sup>-1</sup>. The value is much higher than the other biowaste materials previously reported as adsorbents for the removal of dyes, such as, 85.47 mg g<sup>-1</sup> by skin almond waste [9], 60.42 mg g<sup>-1</sup> by activated carbon from male flowers of coconut tree [14], and 64.87 mg g<sup>-1</sup> by activated carbon prepared from rice husk [16].

### 3.6. Adsorption isotherms modeling

Adsorption data are most commonly represented by the equilibrium isotherm value, which is a plot of the quantity of the sorbate removed per unit sorbent ( $q_{eq}$ ) as the solid phase concentration of the sorbate against the concentration of the sorbate in the liquid phase ( $C_{eq}$ ). The equilibrium isotherm value is of fundamental importance for the design and optimization of the adsorption system for the removal of a dye from an aqueous solution. Therefore, it is necessary to establish the most appropriate correlation for the equilibrium curve. Several isotherm models have been used to predict validity of the experimental data. In the present study, two of the most commonly used models, namely, the Langmuir and Freundlich isotherms, were used to describe the adsorption equilibrium.

The Langmuir isotherm is based on the assumption of monolayer adsorption on a structurally homogeneous adsorbent, where all the adsorption sites are identical and energetically equivalent, wherein the adsorption occurs at specific homogeneous sites within the adsorbent, and once a dye molecule occupies a site no further adsorption can take place at that site [6]. The intermolecular forces decrease rapidly with distance, and consequently the existence of monolayer coverage of the adsorbate at the outer surface of the adsorbent can be predicted [21]. The Freundlich isotherm model is an empirical expression that encompasses the heterogeneity of the surface and the exponential distribution of sites and their energies. A comparison of the Langmuir (Fig. 7a) and Freundlich (Fig. 7b) adsorption isotherms shows that the sorption characteristics of CV dye onto GFP followed more closely the Langmuir isotherm equation (Eq. (3)) than the Freundlich isotherm equation (Eq. (4)). This observation is further supported by the closer to unity value of their respective correlation coefficients ( $r^2$ ), which is a measure of how well the predicted values from a forecast model match with the experimental data [29]. The adsorption parameters of CV on GFP for Langmuir and Freundlich constants are given in Table 1. The  $r^2$  value in respect of sorption of CV for Langmuir isotherm model was noted to be 0.994, which for Freundlich isotherm model was 0.974. It may be concluded from these observations that the adsorption of CV by GFP was better defined by the Langmuir than by the Freundlich equation thus indicating that the adsorption of CV onto GFP is a chemically equilibrated and saturated mechanism. The maximum CV binding capacity of GFP was found to be 249.68 mg g<sup>-1</sup> and was consistent with the experimental data (Table 1). This adsorption capacity of GFP for CV was also found to be significantly higher in comparison with some other recently reported adsorbents, such as 85.47 mg g<sup>-1</sup> by skin almond waste [30], 64.87 mg g<sup>-1</sup> by activated rice husk [16], and 113 mg g<sup>-1</sup> by activated sludge [31].

**Table 1**  
The Langmuir and Freundlich isotherms model constants, and their respective correlation coefficients ( $r^2$ ) for the sorption of crystal violet from aqueous solution by grapefruit peel.

Experimental (mg g <sup>-1</sup> )	Langmuir			Freundlich		
	$q_{max}$ (mg g <sup>-1</sup> )	$b$ (L mg <sup>-1</sup> )	$r^2$	$K_F$	$1/n$	$r^2$
254.16 ± 6.86	249.68	0.131	0.994	3.14	0.446	0.974

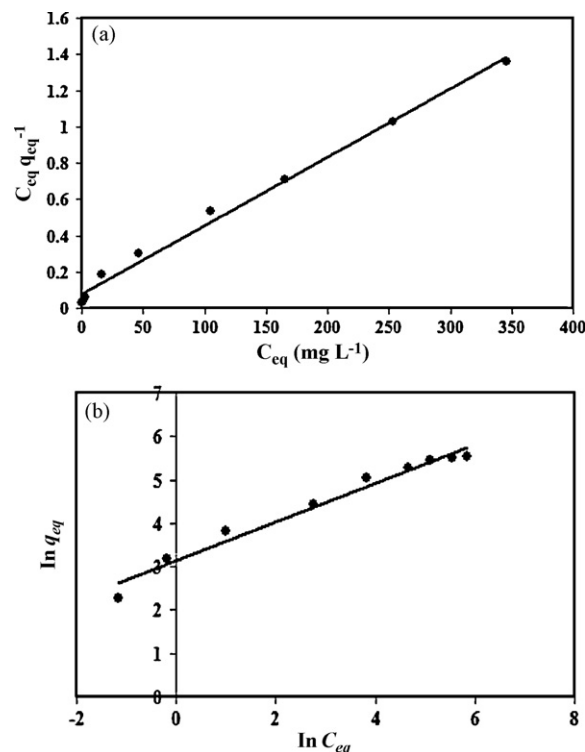


**Fig. 7.** The linearized (a) Langmuir and (b) Freundlich adsorption isotherms for the sorption of crystal violet by grapefruit peel.

**Table 2**  
Characteristics of the Langmuir adsorption isotherms.

Separation factor ( $R_L$ )	Type of isotherms
$R_L > 1$	Unfavourable
$R_L = 1$	Linear
$0 > R_L > 1$	Favourable
$R_L = 0$	Irreversible

The Langmuir parameters can also be used to predict affinity between the sorbate and the sorbent using the dimensionless separation factor ( $R_L$ ), which has been defined as below [32]:

$$R_L = \frac{1}{1 + bC_i} \quad (8)$$

The value of  $R_L$  can be used to predict whether a sorption system is “favourable” or “unfavourable” in accordance with the criteria shown in Table 2. The value of  $R_L$  for the sorption of CV onto GFP is shown in Fig. 8, which indicates that sorption of CV on GFP was “favourable”.

### 3.7. Kinetics modeling

To examine the controlling mechanism of the adsorption process, such as mass transfer and chemical reaction, the pseudo-first-order and the pseudo-second-order kinetics models were used to test the experimental data of dye adsorption by GFP. The

**Table 3**

Theoretically determined constants of the pseudo-first and the pseudo-second-order reaction kinetics based on the sorption of crystal violet from 25 mg L<sup>-1</sup> solutions, pH 6.0, by 1.0 g L<sup>-1</sup> grapefruit peel during shake flask sorbent–sorbate contact at 100 rpm for 240 min.

Experimental $q_{eq}$ (mg g <sup>-1</sup> )	Pseudo-first-order constants			Pseudo-second-order constants		
	$q_{eq}$ (mg g <sup>-1</sup> )	$k_1$ (min <sup>-1</sup> )	$r^2$	$q_{eq}$ (mg g <sup>-1</sup> )	$k_2$ (g mg <sup>-1</sup> min <sup>-1</sup> )	$r^2$
24.05	8.84	-0.031	0.838	24.31	0.005	0.992

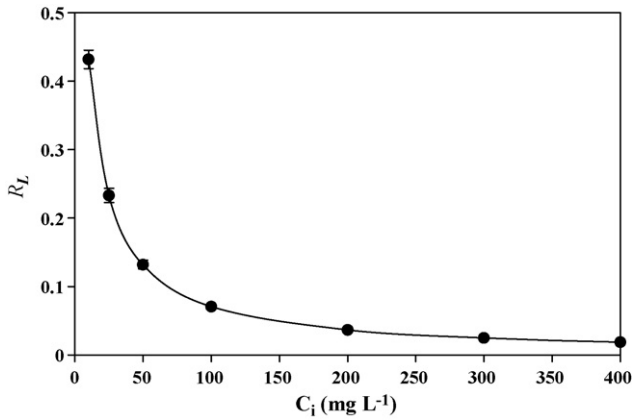


Fig. 8. Value of separation factor  $R_L$  for sorption of crystal violet by grapefruit peel.

experimental data for the removal of CV when analyzed on the pseudo-first-order equation (Eq. (5)) did not result in a perfect straight line when a plot was drawn between  $\ln(q_{eq} - q_t)$  and  $t$  indicating a non-fit on the model (Fig. 9a). A good linear plot of  $t/q_t$  against  $t$  for the pseudo-second-order kinetics model (Eq. (6)) shows a fit on the model (Fig. 9b). Kinetics parameters for the sorption of CV by GFP, as calculated from the linear plots of the

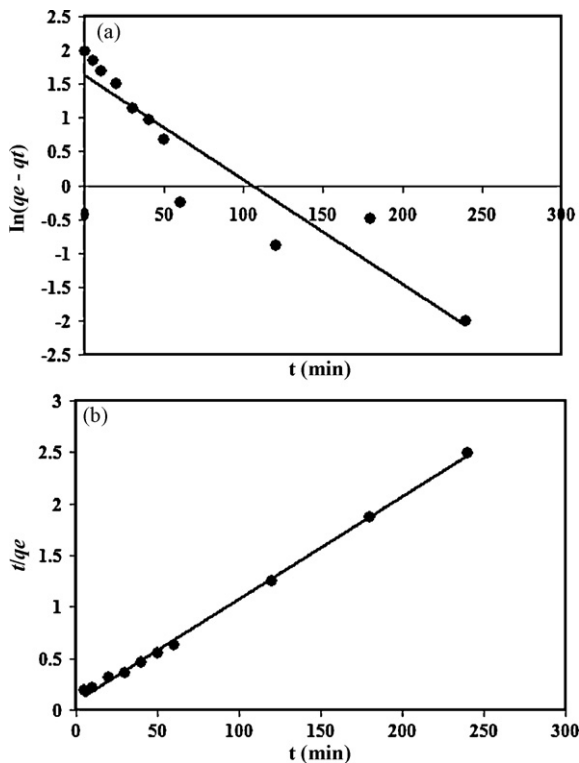


Fig. 9. Linearized (a) pseudo-first-order and (b) pseudo-second-order plots for the sorption of crystal violet by grapefruit peel waste.

pseudo-first-order (Fig. 9a) and the pseudo-second-order (Fig. 9b) kinetics models are presented in Table 3. The low correlation coefficient value ( $r^2 = 0.838$ ), as obtained for the pseudo-first-order model, indicates that sorption of CV did not follow the pseudo-first-order reaction. The insufficiency of the pseudo-first-order model to fit the kinetics data could possibly be due to the limitations of the boundary layer controlling the sorption process. The experimental data were observed to fit well the pseudo-second-order equation. The high correlation coefficient value ( $r^2 = 0.992$ ), as obtained for the linear plot of  $t/q_t$  against  $t$  for the pseudo-second-order equation, was observed to be close to 1. This suggests that the process of sorption kinetics of CV by GFP follows the pseudo-second-order equation and the process controlling the rate may be controlled by chemical sorption involving valence forces through sharing or exchange of electrons between sorbent and sorbate [24].

### 3.8. Proposed sorption mechanism

The pattern of adsorption onto plant materials is attributable to the active groups and bonds present on them [33]. For the elucidation of these active site, FTIR spectrophotometry was performed. Peaks appearing in the FTIR spectrum of GFP (Fig. 10) were assigned to various groups and bonds in accordance with their respective wavenumbers (cm<sup>-1</sup>) as reported in literature. The region between 2600 cm<sup>-1</sup> and 3600 cm<sup>-1</sup> shows two major band stretches. A broad and strong band stretch was observed from 3000 cm<sup>-1</sup> to 3600 cm<sup>-1</sup>, indicating the presence of free or hydrogen bonded O–H groups (alcohols, phenols and carboxylic acids) as in pectin, cellulose and lignin on the surface of the adsorbent [34]. The O–H stretching vibrations occur within a broad range of frequencies indicating the presence of “free” hydroxyl groups and bonded O–H bands of carboxylic acids. The light stretch at 2909.64 cm<sup>-1</sup> showed the stretching of symmetric or asymmetric C–H vibration of aliphatic acids [35]. The peak observed at 1730 cm<sup>-1</sup> is the stretching vibration of C=O bond due to non-ionic carboxyl groups (–COOH, –COOCH<sub>3</sub>) and may be assigned to carboxylic acids or their esters [36]. Asymmetric and sym-

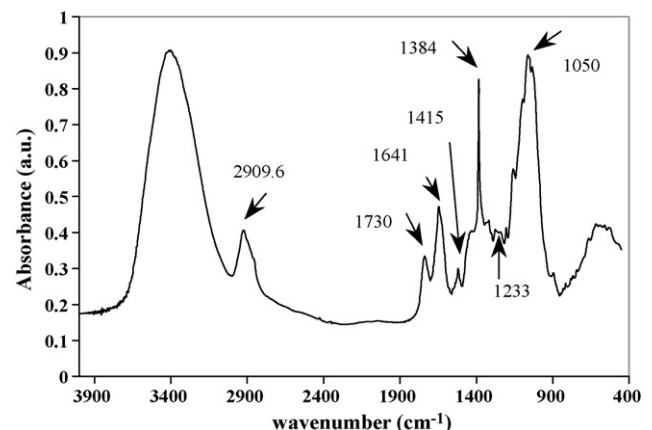


Fig. 10. FTIR spectra of native grapefruit peel waste.

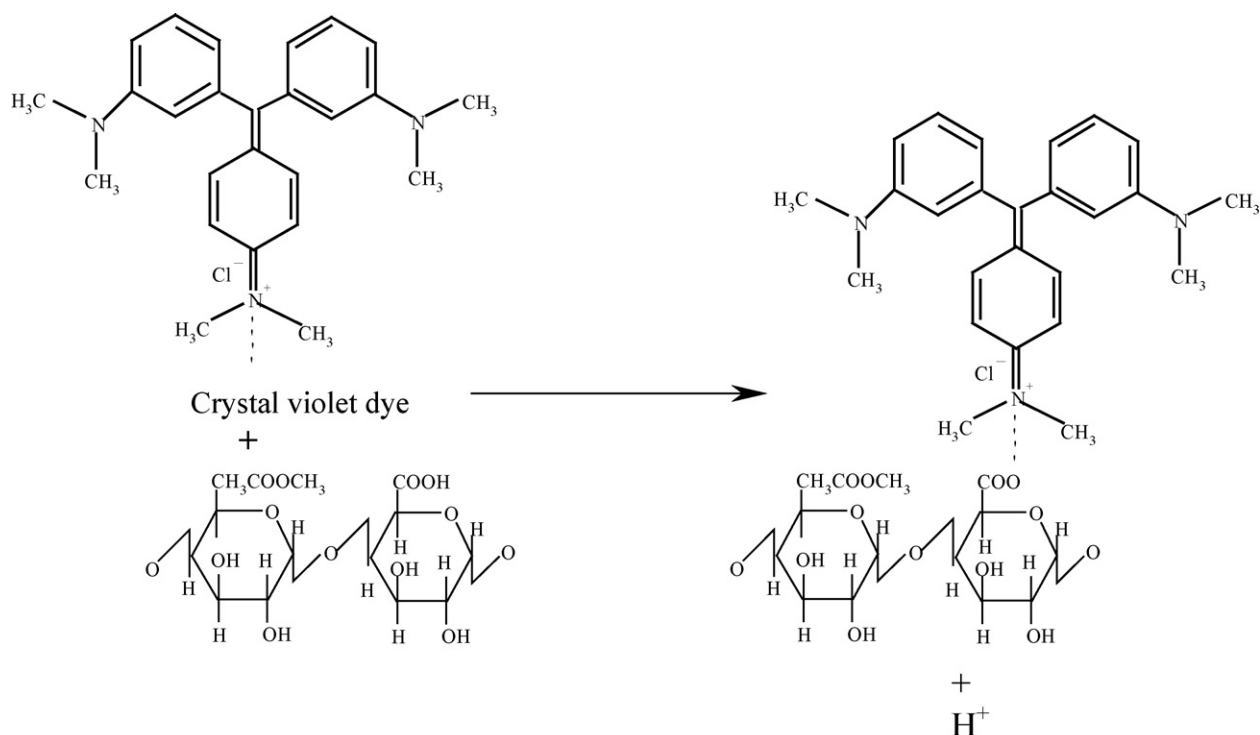


Fig. 11. Proposed ion exchange mechanism between a proton of grapefruit peel waste and crystal violet dye.

metric stretching vibrations of ionic carboxylic groups ( $-\text{COO}^-$ ), respectively, appeared at  $1641\text{ cm}^{-1}$  and  $1415\text{ cm}^{-1}$ . The peaks at  $1384\text{ cm}^{-1}$  may be assigned to symmetric stretching of  $-\text{COO}^-$  of pectin [36], and aliphatic acids group vibration at  $1233\text{ cm}^{-1}$  to deformation vibration of  $\text{C}=\text{O}$  and stretching formation of  $-\text{OH}$  of carboxylic acids and phenols [37], and at  $1050\text{ cm}^{-1}$  can be assigned to the stretching vibration of  $\text{C}-\text{OH}$  of alcoholic groups and carboxylic acids [37]. It is well indicated from the FTIR spectrum of GFP that carboxyl and hydroxyl groups were present in abundance. The sorption of CV on the GFP biomass may likely be due to the electrostatic attraction between these groups and the cationic dye molecule ( $\text{CV}^+$ ). At pH above 4, the carboxylic groups are deprotonated and negatively charged carboxylate ligands ( $-\text{COO}^-$ ) bind the positively charged CV molecules. This confirms that the sorption of CV by GFP was an ion exchange mechanism between the negatively charged groups present in the cell wall of GFP and the cationic dye molecule. The proposed mechanism of sorption of CV by GFP is shown in Fig. 11.

### 3.9. Desorption of CV from GFP

Recovery of CV from exhausted biomass of GFP and regeneration of GFP was tested by using aqueous solution of 1 M NaOH [37]. For the purpose, 1 g of CV-loaded GFP was contacted with 50 mL of 1 M NaOH and shaken at 100 rpm on a rotary shaker at  $30^\circ\text{C}$ . The kinetics of desorption of CV from the CV-loaded GFP is shown in Fig. 12. It may be noted that CV desorbed very rapidly, with the maximum elution achieved in the first 30 min amounting to 82% desorption. The desorption rate after this initial fast phase, however, was observed to slow down significantly until it reached a plateau after 60 min, indicating equilibrium of the system. The desorption efficiency was 98.25%. The regenerated GFP biomass was again used for removal of CV and was found to have the efficiency of 87% and 81% in the second and the third cycles, respectively. Similar observations for the desorption of CV from surfactant-modified alumina using NaOH have been reported

[38]. The successful recovery of CV at >98% using 1 M NaOH from the CV-loaded GFP and the high sorption  $q_{\text{max}}$  of  $254.16\text{ mg g}^{-1}$  of GFP, coupled with the use of a no cost industrial waste as an adsorbent, indicate that the material reported in the present study has a good potential for the removal of the dye from wastewaters.

### 3.10. CV removal by GFP from made-up wastewater in fixed-bed continuous-flow column

The potential shown by GFP to remove CV from aqueous solution in shake flask studies was further tested in a fixed-bed continuous-flow column using made-up wastewater. For this purpose, CV was added to tapwater at the known concentrations of  $50\text{ mg L}^{-1}$  and  $100\text{ mg L}^{-1}$  and passed through the separate columns packed with  $14 \pm 0.56\text{ g}$  of GFP. The breakthrough biosorption curves are presented in Fig. 13. The dye loading curve showed an excellent clear zone (100% removal) before the breakthrough point. The results presented in Fig. 13 show that the column bioreactor packed with  $14 \pm 0.56\text{ g}$  GFP had the capacity to treat 61 L and 29 L dye solution before reaching the breakthrough point for  $50\text{ mg L}^{-1}$

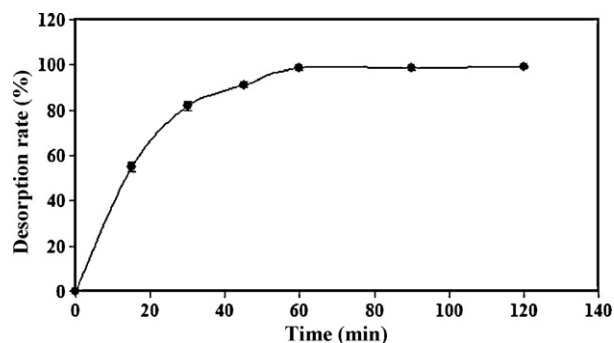


Fig. 12. Desorption kinetics of crystal violet from GFP.

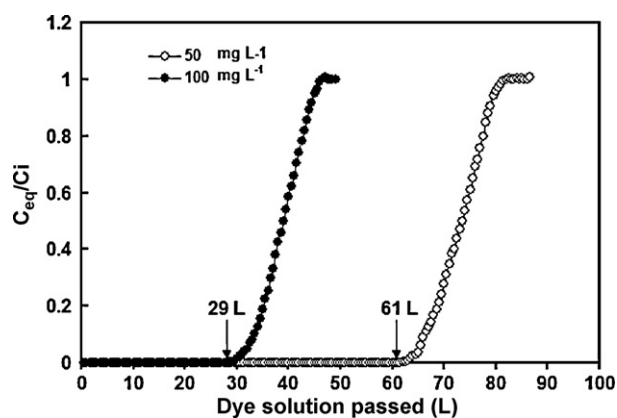


Fig. 13. Breakthrough curves of biosorption of crystal violet by grapefruit peel waste in fixed-bed continuous-flow column.

and  $100 \text{ mg L}^{-1}$  CV, respectively, and the saturation points were achieved at 83 L and 45 L (Fig. 13). The total biosorption capacity of the packed column bioreactor was calculated by integrating the breakthrough curves between the breakthrough and saturation points. The breakthrough point of the GFP-packed column is the point at which CV concentration in the effluent (outlet dye concentration) reached at concentration above zero whereas the saturation point is the time at which CV concentration in the effluent become equal to inlet dye concentration. The sorption capacity of GFP for  $50 \text{ mg L}^{-1}$  and  $100 \text{ mg L}^{-1}$  CV, respectively, was calculated to be  $259.91 \text{ mg g}^{-1}$  and  $266.15 \text{ mg g}^{-1}$ , which is even better than the maximum value of  $254.16 \text{ mg g}^{-1}$  obtained during batch-scale studies.

#### 4. Conclusions

Studies suggest that GFP can be effectively used as a cost-effective adsorbent for removal of CV from aqueous solution. Batch adsorption studies show that removal is dependent upon process parameters like pH, sorbate and sorbent concentrations and contact time. Sorption followed pseudo-second-order kinetics equation. The experimental equilibrium sorption data obtained from batch studies at optimized conditions fit well to Langmuir adsorption isotherm equation, indicating monolayer adsorption. The dimensionless parameter  $R_L$  has also been calculated using the Langmuir constant  $b$ . The values of  $R_L$  have been found to be between 0 and 1 which again suggest favourable adsorption. FTIR analysis showed that the main functional sites taking part in the sorption of CV included carboxyl and hydroxyl groups. GFP could be regenerated and could be reused. Column studies have shown that GFP can be used efficiently for continuous removal of CV. The present study concludes that the GFP could be employed as low-cost adsorbent as an alternative to commercial activated carbon for the removal of colour and dyes from water and wastewater, in general and for the removal of CV in particular.

#### Acknowledgements

Asma Saeed acknowledges project grant no. W/3781-2 by International Foundation for Science, Stockholm, Sweden awarded in collaboration with COMSTECH, Islamabad, Pakistan, and Mehwish Sharif acknowledges financial support from Higher Education Commission (HEC), Islamabad, Pakistan, project NRP-707 granted to Dr. Saeed Iqbal Zafar, HEC Eminent Researcher, to whom both are further thankful for his guidance throughout the course of the present study.

#### References

- [1] A. Bhatnagar, A.K. Jain, M.K. Mukul, Removal of congo red dye from water using carbon slurry waste, *Environ. Chem. Lett.* 2 (2005) 199–202.
- [2] Z. Aksu, Application of biosorption for the removal of organic pollutants: a review, *Process Biochem.* 40 (2005) 997–1026.
- [3] C.K. Lee, K.S. Low, P.Y. Gan, Removal of some organic dyes by acid treated spent bleaching earth, *Environ. Technol.* 20 (1999) 99–104.
- [4] M. Ramakrishnan, S. Nagarajan, Utilization of waste biomass for the removal of basic dye from water, *World Appl. Sci. J.* 5 (2009) 114–121.
- [5] S.D. Khattri, M.K. Singh, Colour removal from synthetic dye wastewater using a biosorbent, *Water Air Soil Pollut.* 120 (2000) 283–294.
- [6] P. Monash, G. Pugazhenthil, Adsorption of crystal violet dye from aqueous solution using mesoporous materials synthesized at room temperature, *Adsorption* 15 (2009) 390–405.
- [7] H. Ali, S.K. Muhammad, Biosorption of crystal violet from water on leaf biomass of *Calotropis procera*, *J. Environ. Sci. Technol.* 1 (2008) 143–150.
- [8] Y. Fu, T. Viraraghavan, Removal of congo red from aqueous solution by fungus *Aspergillus niger*, *Adv. Environ. Res.* 7 (2002) 239–247.
- [9] F. Atmani, A. Bensmaili, N.Y. Mezener, Synthetic textile effluent removal by skin almonds waste, *J. Environ. Sci. Technol.* 2 (2009) 53–169.
- [10] E. Lorenc-Grabowska, E. Gryglewicz, Adsorption characteristics of congo red on coal based mesoporous activated carbon, *Dyes Pigments* 74 (2007) 34–40.
- [11] C.C. Chen, H.J. Liao, C.Y. Cheng, C.Y. Yen, Y.C. Chung, Biodegradation of crystal violet by *Pseudomonas putida*, *Biotechnol. Lett.* 29 (2007) 391–396.
- [12] O. Gezici, M. Küçükosmanoğlu, A. Ayar, The adsorption behaviour of crystal violet in functionalized sporopollenin-mediated column arrangements, *J. Colloid Interface. Sci.* 304 (2006) 307–316.
- [13] F. Akbal, Adsorption of basic dyes from aqueous solution onto pumice powder, *J. Colloid Interface Sci.* 286 (2005) 455–458.
- [14] S. Senthilkumar, P. Kalaamani, C.V. Subbaram, Liquid phase adsorption of crystal violet onto activated carbons derived from male flowers of coconut tree, *J. Hazard. Mater.* 136 (2006) 800–808.
- [15] V. Meshko, L. Markovska, M. Mincheva, A.E. Rodrigues, Adsorption of basic dyes on granular activated carbon and natural zeolite, *Water Res.* 33 (2001) 3357–3366.
- [16] K. Mohantay, J.T. Naidu, B.C. Meikap, M.N. Biswas, Removal of crystal violet from wastewater by activated carbons prepared from rice husk, *Ind. Eng. Chem. Res.* 45 (2006) 5165–5171.
- [17] USDA/NASS/FFO, Citrus Summary 2006–07. United States Department of Agriculture, National Agricultural Statistics Service and Florida Field Office, Orlando, Florida, USA, 2008, p. 55.
- [18] M.R. Wilkins, W. Widmer, K. Grohmann, R.G. Cameron, Hydrolysis of grapefruit peel waste with cellulase and pectinase enzymes, *Bioresour. Technol.* 98 (2007) 1596–1601.
- [19] S.V. Ting, E.J. Deszyck, The carbohydrates in the peel of oranges and grapefruit, *J. Food Sci.* 26 (1961) 146–152.
- [20] R.S. Blackburn, Natural Polysaccharides, Their interactions with dye molecules: applications in effluent treatment, *Environ. Sci. Technol.* 38 (2004) 4905–4909.
- [21] I. Langmuir, The adsorption of gases on plane surfaces of glass, mica, and platinum, *J. Am. Chem. Soc.* 40 (1918) 1361–1403.
- [22] H.M.F. Freundlich, Über die adsorption in lösungen, *Z. Physikalische Chem. (Leipzig)* 57A (1906) 385–470.
- [23] S. Lagergren, Zur theorie der sogenannten adsorption gelösterstoffe, *Kungliga Svenska Vetenskapsakademiens, Handlingar* 24 (1898) 1–39.
- [24] Y.S. Ho, G. Mackay, Sorption of dye from aqueous solution by peat, *Chem. Eng. J.* 70 (1998) 115–124.
- [25] Y.S. Ho, Effect of pH on lead removal from water using tree fern as the sorbent, *Bioresour. Technol.* 96 (2005) 1292–1296.
- [26] S.I. Zafar, M. Bisma, A. Saeed, M. Iqbal, FTIR spectrophotometry, kinetics and adsorption isotherms modeling, and SEM-EDX analysis for describing mechanism of biosorption of the cationic basic dye methylene blue by a new biosorbent (sawdust of silver fir; *Abies pindrow*), *Fresen. Environ. Bull.* 17 (2008) 2109–2121.
- [27] A. Saeed, M. Iqbal, S.I. Zafar, Immobilization of *Trichoderma viride* for enhanced methylene blue biosorption: batch and column studies, *J. Hazard. Mater.* 168 (2009) 406–415.
- [28] M. Iqbal, A. Saeed, Biosorption of reactive dye by loofa sponge-immobilized fungal biomass of *Phanerochaete chrysosporium*, *Process Biochem.* 42 (2007) 1160–1164.
- [29] M. Iqbal, A. Saeed, S.I. Zafar, FTIR spectrophotometry, kinetics and adsorption isotherms modeling, ion exchange, and EDX analysis for understanding the mechanism of  $\text{Cd}^{2+}$  and  $\text{Pb}^{2+}$  removal by mango peel waste, *J. Hazard. Mater.* 164 (2009) 161–171.
- [30] F. Atmani, A. Bensmaili, N.Y. Mezener, Synthetic textile effluent removal by skin almond waste, *J. Environ. Sci. Technol.* 2 (2009) 153–169.
- [31] H.C. Chu, K.M. Chen, Reuse of activated sludge biomass: I. Removal of basic dyes from wastewater by biomass, *Process Biochem.* 37 (2002) 595–600.
- [32] K.R. Hall, L.C. Eagleton, A. Acrivos, T. Vermeulen, Pore and solid diffusion kinetics in fixed bed adsorption under constant-pattern conditions, *Ind. Eng. Chem. Fundam.* 5 (1996) 212–223.
- [33] K.K. Krishnani, M.X. Xiaoguang, C. Christodoulatos, V.M. Boddu, Biosorption mechanism of nine different heavy metals onto biomatrix from rice husk, *J. Hazard. Mater.* 153 (2008) 1222–1234.



- [34] R. Gnanasambandam, A. Protor, Determination of pectin degree of esterification by diffuse reflectance Fourier transform infrared spectroscopy, *Food Chem.* 68 (2000) 327–332.
- [35] F.T. Li, H. Yang, Y. Zhao, R. Xu, Novel modified pectin for heavy metal adsorption, *Chin. Chem. Lett.* 18 (2007) 325–328.
- [36] N.V. Farinella, G.D. Matos, M.A.Z. Arruda, Grape bagasse as a potential biosorbent of metals in effluent treatment, *Bioresour. Technol.* 98 (2007) 1940–1946.
- [37] G. Guibaud, N. Tixier, A. Bouju, M. Baudu, Relationship between extracellular polymer's composition and its ability to complex Cd, Cu and Ni, *Chemosphere* 52 (2003) 1701–1710.
- [38] A. Adak, M. Bandyopadhyay, A. Pal, Removal of crystal violet dye from wastewater by surfactant-modified alumina, *Sep. Purif. Technol.* 44 (2005) 139–144.